A comparison of generative models for the detection and identification of gaseous chemical plumes in hyperspectral imagery

Brandyn Ward

University of California, Santa Cruz

Abstract

We focus on comparing a class of semi-supervised generative methods as they are the most applicable (and most used) for realistic data scenarios in the remote sensing of gaseous plumes through hyperspectral imagery. The methods we compare within this class are three regression models□spectral matched filter (SMF), endmember selection (EMS), and least absolute shrinkage and selection operator (LASSO)□and one Bayesian model□Bayesian adaptive spline surfaces (BASS). In our validations through fitting these methods on two semi-synthetic hyperspectral images, we find that the LASSO model provides the most robust inference, closely followed by the SMF model adapted through an elliptically contoured generalized likelihood ratio test (EC-GLRT) filter.

Hyperspectral Imagery

Hyperspectral imagery data is gathered using a hyperspectral sensor, which is a spectrometer specifically engineered to measure the radiance of incoming electromagnetic waves across many (typically several tens to hundreds) equidistant, narrow (0.01μm−0.1μm) spectral bands. The data and image are arranged in such a way to form a cube: the pixels (spatial dimensions) of the image are represented by the x and y coordinate axes, while the spectral dimension is expressed through the z-axis (Figure 1).

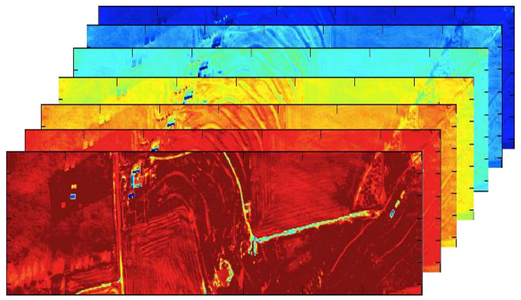

Figure 1: example of the data cube representation for hyperspectral imagery data where each image slice (z-axis) represents a sampled spectra for the same imaged region (x and y axes).

Linear Sensor Model

We use the linear radiative sensor signal model presented in [1] to model the measured radiance across all K spectral bands at a particular hyperspectral pixel, $j \in \{1, \dots, J\}$, given by the K length vector $\mathbf{x}$:

$$\mathbf{x}_j = \sum_{m=1}^{M} g_{m,j}\boldsymbol{s}_m + \mathbf{v} = \mathbf{S}\mathbf{g}_j + \mathbf{v}.$$

Where,

- $g_{m,j} = C_B \Delta T \gamma_{m,j}$ is the abundance
- $\mathbf{s}_m = \{[\tau_a(\boldsymbol{\lambda})\alpha_m(\boldsymbol{\lambda})] * R_F(\boldsymbol{\lambda})\}$ is the chemical signature
- $\mathbf{v} = \{L_{\text{off}}(\boldsymbol{\lambda}) * R_F(\boldsymbol{\lambda})\} + r(\boldsymbol{\lambda}) + n(\boldsymbol{\lambda})$ is the error imposed by the clutter, transmittance linearization, and sensor noise, respectively

Generative Methods

We assume the linear model for our generative methods with $\mathbf{v} \sim N(\mathbf{0}, \boldsymbol{\Sigma}_x)$ through mean shifting each of our pixel observations, $\mathbf{x}_j^* = \mathbf{x}_j - \boldsymbol{\mu}_x$, and using the dominant mode rejection (DMR) estimator of [2] to robustly estimate $\boldsymbol{\Sigma}_x^{-1}$.
The first of the three regression methods we use is the endmember selection (EMS) method,

$$\hat{g}_{m,j}^{(OSP)} = \boldsymbol{d}^T \boldsymbol{P}\mathbf{x}_j = \boldsymbol{d}^T \boldsymbol{P}\boldsymbol{d}_{g_{m,j}} + \boldsymbol{d}^T \boldsymbol{P}\mathbf{v}.$$

Which attempts to bolster the desired signal, $\boldsymbol{d}$, in the provided spectral chemical library, $\mathbf{S}$, by applying a matched filter and projecting out the rest of the library, $\mathbf{U}$, through the ordinary least squares (OLS) projection operator, $\boldsymbol{P} = \mathbf{I} - \mathbf{U}(\mathbf{U}^T\mathbf{U})^{-1}\mathbf{U}^T$.
Secondly, the spectral matched filter (SMF) method uses the weighted least squares estimator for each of the regression coefficients:

$$\hat{\mathbf{g}}_j^{(SMF)} = \left(\mathbf{S}^T\boldsymbol{\Sigma}_{\text{DMR}}^{-1}\mathbf{S}\right)^{-1}\mathbf{S}^T\boldsymbol{\Sigma}_{\text{DMR}}^{-1}\mathbf{x}_j.$$

If $\boldsymbol{\Sigma}_x^{-1}$ departs from Gaussianity, we use the elliptically-contoured generalized likelihood ratio test (EC-GLRT) filter proposed by [3] to recover closer to optimal results in the presence of heavily non-linear clutter,

$$\hat{\mathbf{g}}_j^{(SMF)} = \sqrt{\frac{(\nu-1)}{(\nu-2)+\mathbf{x}_j^T\boldsymbol{\Sigma}_{\text{DMR}}^{-1}\mathbf{x}_j}}\left(\mathbf{S}^T\boldsymbol{\Sigma}_{\text{DMR}}^{-1}\mathbf{S}\right)^{-\frac{1}{2}}\mathbf{S}^T\boldsymbol{\Sigma}_{\text{DMR}}^{-1}\mathbf{x}_j.$$

Here, $\mathbf{v}$ is assumed to be distributed as a t-distribution with $\nu = \mathcal{O}(K)$ degrees of freedom (DOF).
The last regression method we use is the least absolute shrinkage and selection operator (LASSO) in which we seek to minimize

$$\min_{\mathbf{g}_j}\left\{\sum_{k=1}^{K}\left(\tilde{x}_{k,j} - \tilde{\mathbf{s}}_k\mathbf{g}_j\right)^2 + \lambda_j\sum_{m=1}^{M}|g_{m,j}|\right\},$$

for each of our regression coefficients where λ_j is the penalization coefficient for the jth pixel.
We then use a standard K-means clustering algorithm to provide a non-parametric decision boundary to classify each of our calculated regression coefficients as either coming from noise (clutter) or signal (gas). We assume the cluster that is larger and has mean nearest zero to be the noise cluster (Figure 2).

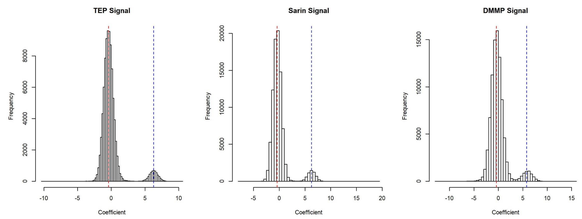

Figure 2: Histograms of the fitted coefficients across all pixels resulting from the SMF model. The K-means clustering algorithm is used to predict the clustering (pixels) of the noise signal, with mean corresponding to the red-dashed line, and chemical signal, mean corresponding to the blue-dashed line.

Lastly, we use a Bayesian adaptive spline surface (BASS) method [4],

$$x_{ij} = f(\mathbf{s}_i) + \epsilon_i, \qquad \epsilon_i \sim N(0, \sigma^2),$$

$$f(\mathbf{s}_i) = a_0 + \sum_{m=1}^{M} a_m B_m(\mathbf{s}_i),$$

$$B_m(\mathbf{s}_i) = \prod_{z=1}^{Z_m} g_{zm}[c_{zm}(s_{v_{zm}} - t_{zm})]_+^{\alpha}.$$

Simulations

We use two semi-synthetic images to evaluate the performance of our methods. The first image (Figure 1) is of resolution 128×700 ($J = 89{,}600$ pixels) across $K = 85$ spectral bands. The second image (Figure 3) is from the MIT Lincoln Laboratory challenge image set of 2014. This image is of resolution 150×320 ($J = 48{,}000$ pixels) across $K = 129$ spectral bands and contains three chemical plumes. Two metrics are used to assess the performance of our methods on the images: the accuracy (ACC) and Matthew's correlation coefficient (MCC). These results are presented in Tables 1 and 2. We also use combined pixel classification masks to visualize pixel inference with respect to the original image. Figure 4 contains these masks for the challenge image.

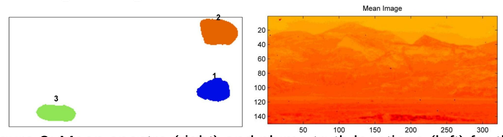

Figure 3: Mean spectra (right) and plume truth locations (left) for the "GID_Targ_Mix_JH" image provided in the MIT Lincoln Lab hyperspectral challenge set.

Tables 1 and 2: ACC and MCC performance metrics for the fit of our methods to the Benchmark image (left) and the "GID_Targ_Mix_JH" MIT challenge image (right).

Model	ACC	MCC
SMF	0.9940	0.9707
EMS	0.9940	0.9707
LASSO	0.9986	0.9927
BASS	0.9690	0.8355

Model	ACC	MCC
SMF	0.2992	0.0848
EMS	0.2031	0.0426
LASSO	0.6796	0.1282
BASS	0.0974	0.0295

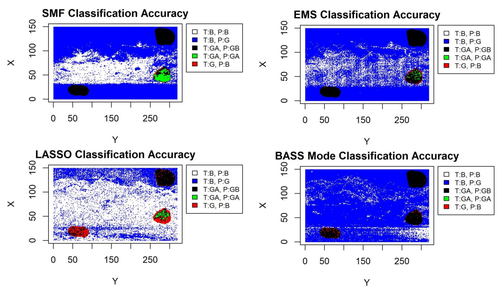

Figure 4: Combined classification masks for each method fitted to the challenge image where five prediction classifications exist: (1) ``T:B, P:B", correctly predicted background pixel, (2) ``T:B, P:G", false-positive, (3) ``T:GA, P:GB", incorrect gas species, (4) ``T:GA, P:GA", correct gas species, and (5) ``T:G, P:B", false-negative.

Discussion

LASSO provides the most robust inference across both images studied with the EC-GLRT adaptation of the SMF following close behind. The EC-GLRT filter provides better inference for plume 1 of the challenge image than LASSO. Additionally, SMF requires less computation time (hundreds of times faster) than LASSO and should be used when time and computational resources are limited. BASS's variable selection properties are lacking, performing the worst.

References

[1] D. Manolakis, S. E. Golowich, and R. S. DiPietro, "Long-wave infrared hyperspectral remote sensing of chemical plumes: a focus on signal processing approaches," *Signal Processing Magazine, IEEE*, no. 31, pp. 120-141, 2014
[2] D. Manolakis, R. Lockwood, T. Cooley, and J. Jacobson, "Hyperspectral detection algorithms: use covariances or subspaces?," *Proc.SPIE,* vol. 7457, 2009
[3] J. Theiler and B. R. Foy, "EC-GLRT: Detecting weak plumes in non-Gaussian hyperspectral clutter using an elliptically-contoured generalized likelihood ratio test," IGARSS 2008-2008 *IEEE International Geoscience and Remote Sensing Symposium*, vol. 1, pp. I-221-I-224, July 2008
[4] D. Francom, B. Sansó, A. Kupresanin, and G. Johannesson, "Sensitivity analysis and emulation for functional data using Bayesian adaptive splines," *UCSC School of Engineering*, 2016